Fault strength dependency of natural earthquake-size distribution based on the precise focal mechanism data

SATOSHI MATSUMOTO[1], YOSHIHISA IIO[2], SHINICHI SAKAI[3], AITARO KATO[4]

1: INSTITUTE SEISMOLOGY AND VOLCANOLOGY, KYUSHU UNIV., 2: DISASTER PREVENTION RESEARCH INSTITUTE, KYOTO UNIV., 3: III/GSII, UNIV. OF TOKYO, 4: EARTHQUAKE RESEARCH INSTITUTE, UNIV. OF TOKYO

EGU23-2507

26 April 2023, 08:00–19:00, Hall X2 at board number X2.68.
attendance time is Wednesday, 26 April 2023, 10:45–12:30.

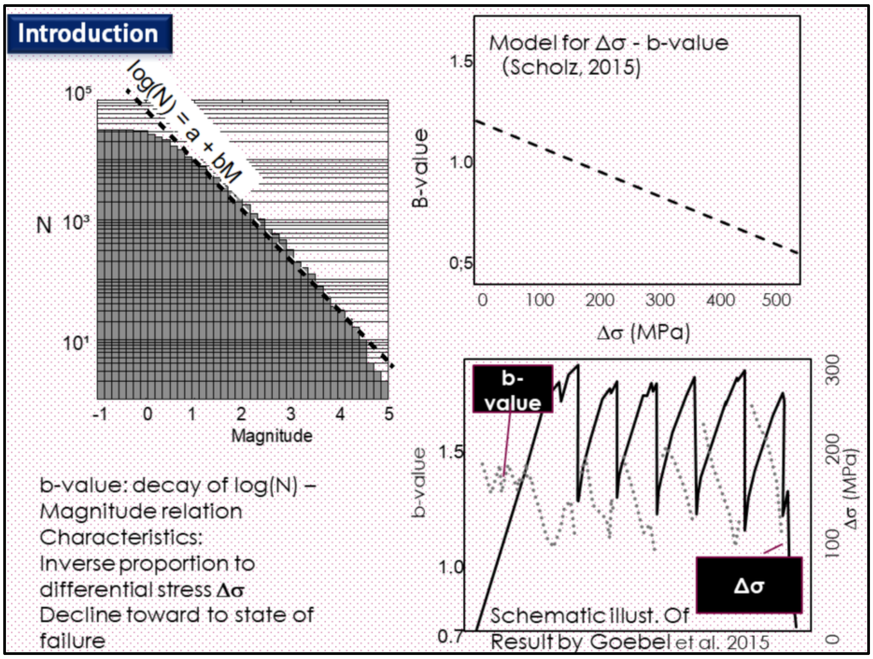

“b-value” is defined as power decay of earthquake magnitude-number distribution. It is famous relation Gutenberg-Richter relation. It means how number of earthquake depends on earthquake size.

According to Scholz 2015, b-value is inversely proportion to the differential stress by investigating natural earthquake sequences for various tectonic setting and depth ranges. In studies through laboratory experiments, there are many results implying b-value decline with stress increasing. In addition, for example Goebel et al., b-value seems to drop toward to failure condition of sample. It suggests that b-value varies due to not only differential stress but also critical condition for fault failure.

AIM

- b-values show temporal and spatial variation. It might be useful to understand state of stress and strength.
- Laboratory experiments reveal the relation between b-value and stress.
- Attempt to find relation of strength – b-value from natural earthquake data.

Method & Data

- Urgent aftershock observation & The 1000 sites seismic observation at the 2000 Western Tottori
- Strength dependency:
  - b-value variation for fault plane orientation
    - Focal mechanism determination
    - Stress field estimation
    - Fault plane selection
    - Normalized Shear and Normal stress estimation and plot on a unit Mohr circle
    - Dividing Mohr circle into parts and estimating b-value

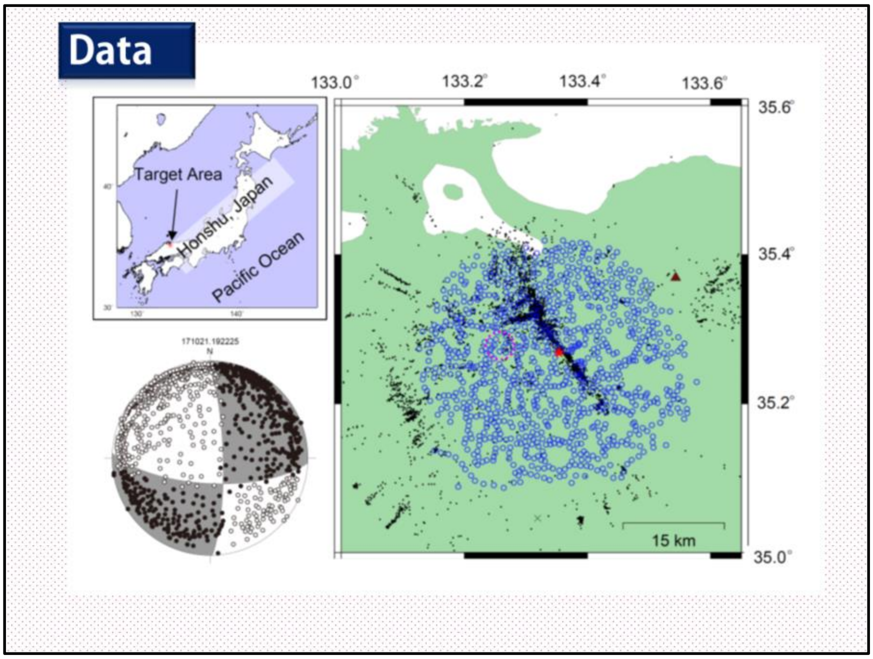

Right) Seismic station geometry of the 2017 Obs. deployed in Southwestern Honshu, Japan shown in index map. Blue open circle and dot indicate seismic station and hypocenter observed by the 2017 Obs. Red star shows epicenter of the 2000 Western Tottori earthquake (M7.2). Solid triangle indicates Daisen volcano. Lower left) An example of focal mechanism solution of the event occurred Oct. 21, 2017 (lower hemisphere plot). Polarity of the first P wave motion of the event is plotted on the lower hemisphere. Solid and open circle indicate positive and negative polarity, respectively.

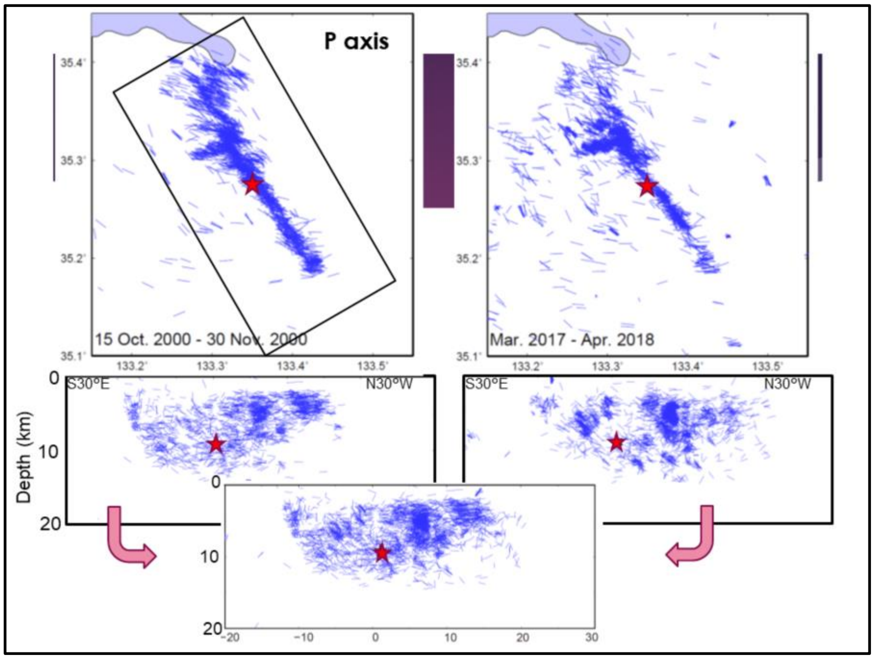

Map and Vertical cross section of P axis distribution for data just after and 18 yrs after the mainshock
Star indicates hypocenter of the mainshock of 2000 Western Tottori earthquake. Stress field and both normalized shear and normal stress for every event are estimated from merged dataset of two observation period.

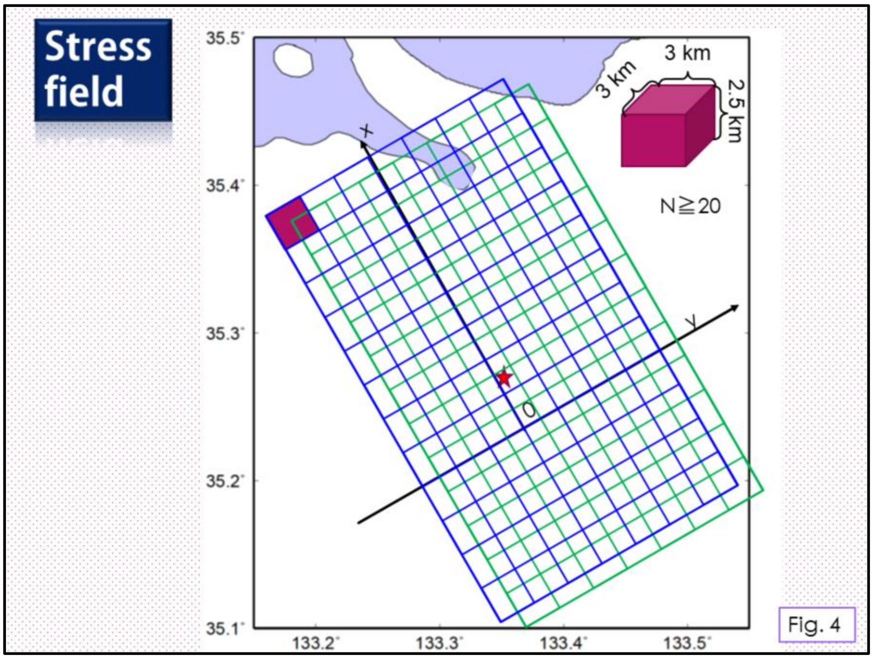

Spatial bin distribution. Size of each bin is 3 x 3 x 2.5 km. Grid distribution is shifted Southwest of half bin size for smoothing stress field. The field is estimated for number of event equal or greater than 20 for each spatial bin. Star indicates epicenter of W-Tottori EQ.

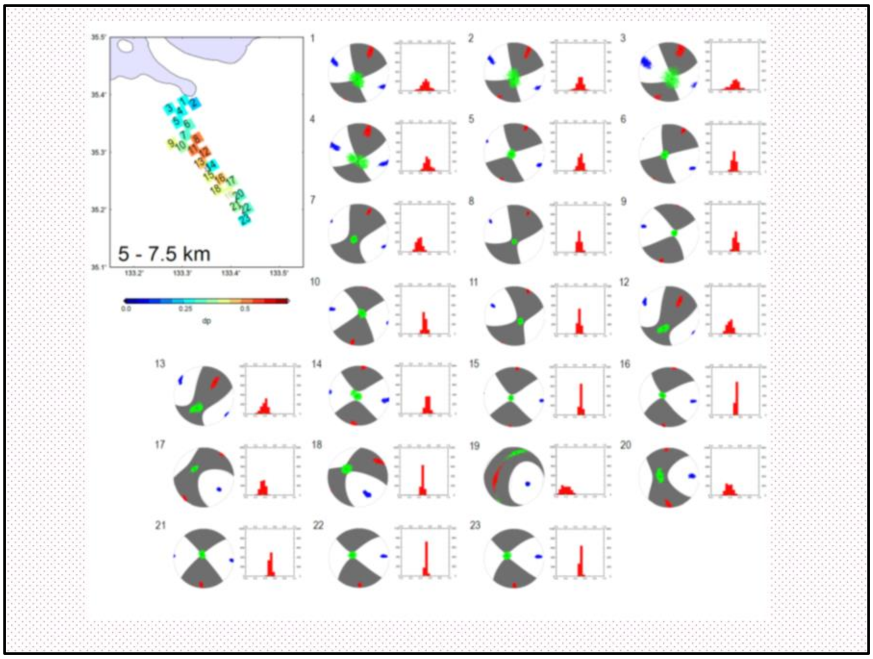

Example stress tensor estimated. Tensor is expressed by focal sphere in lower hemisphere. Blue, green, and red symbols show ranges of 95 % of Max. Mid. Min. principal stresses. confidence range. Histogram shows 95 % range for stress ratio.

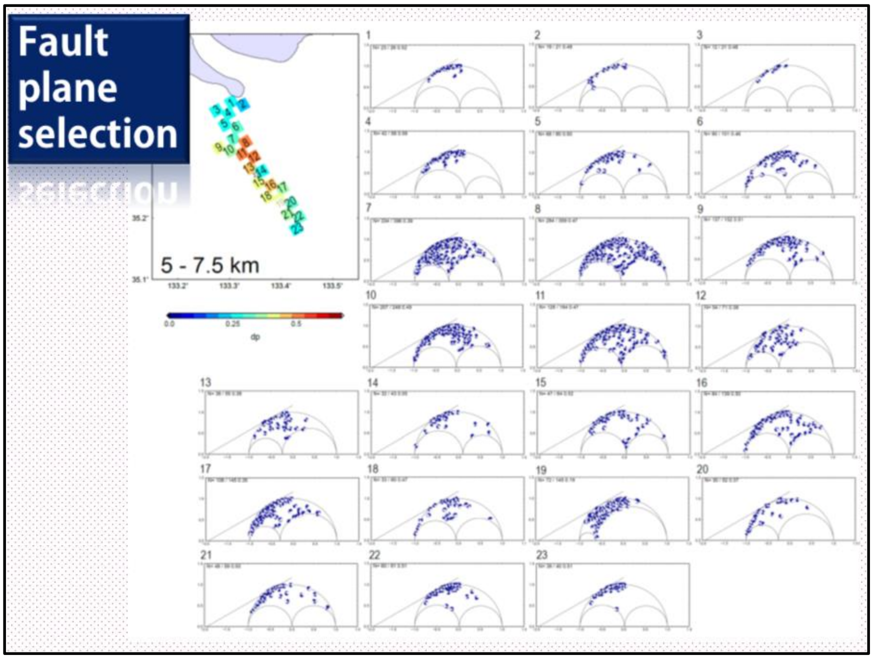

Examples for Shear and normal stress distribution on unit Mohr circles drawn from the estimated stress field in the distributed spatial bins.

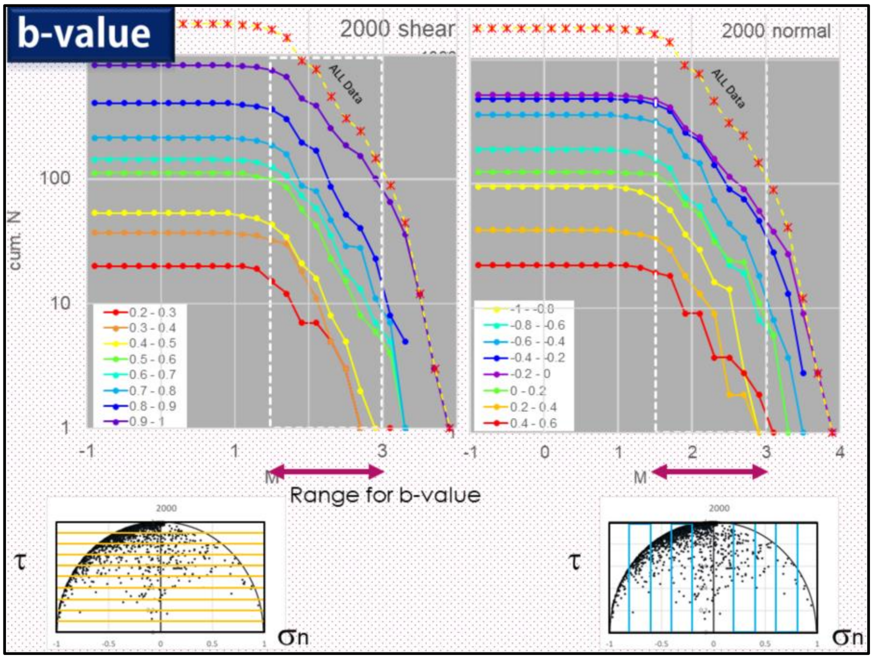

We marge shear and normal stresses for all available (that is estimated stress field) spatial bins.
First, we compare frequency-magnitude distribution for range divided shear and normal stress.
Red arrow displays range for estimating b-value.
This is result for the 2000 obs. Data.

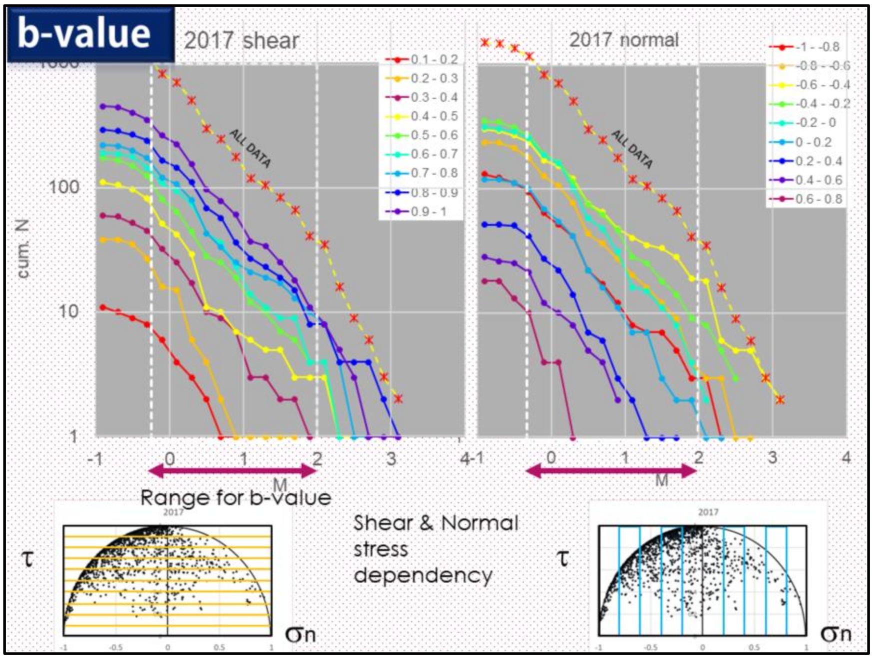

For 2017 obs. Data.

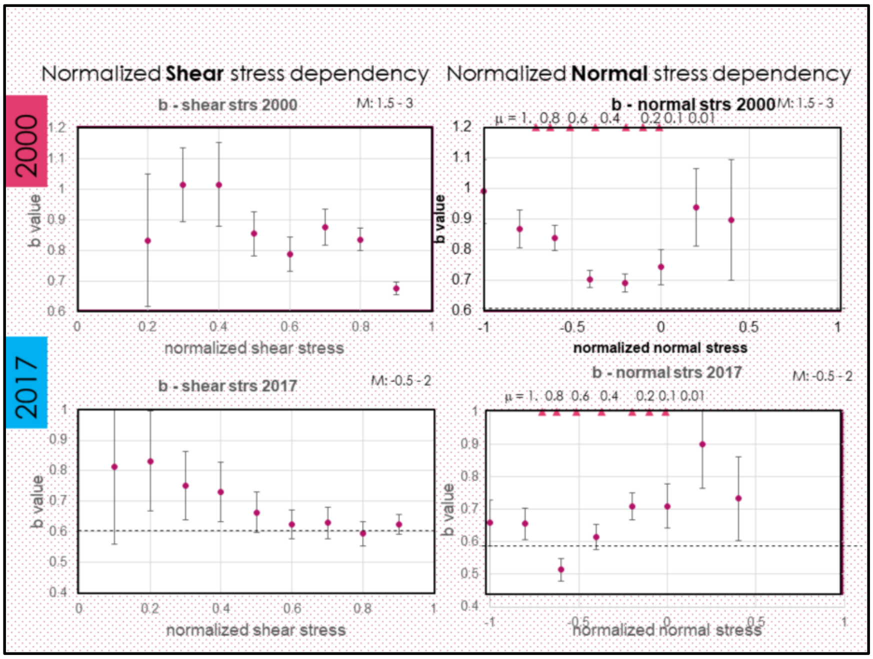

"b-value" plotted for normalized shear (left) and normal (right) stresses. Upper and Lower panels show result for 2000 and 2017 obs. Data. The result shows that the b-value decreases with increasing shear stress. On the other hand, b-value for normal stress variation takes minimum value at -0.2 for 2000 obs. and -0.6. Triangle in right panels indicates friction coefficient that inferred from touching point of Mohr circle and Coulomb failure function.

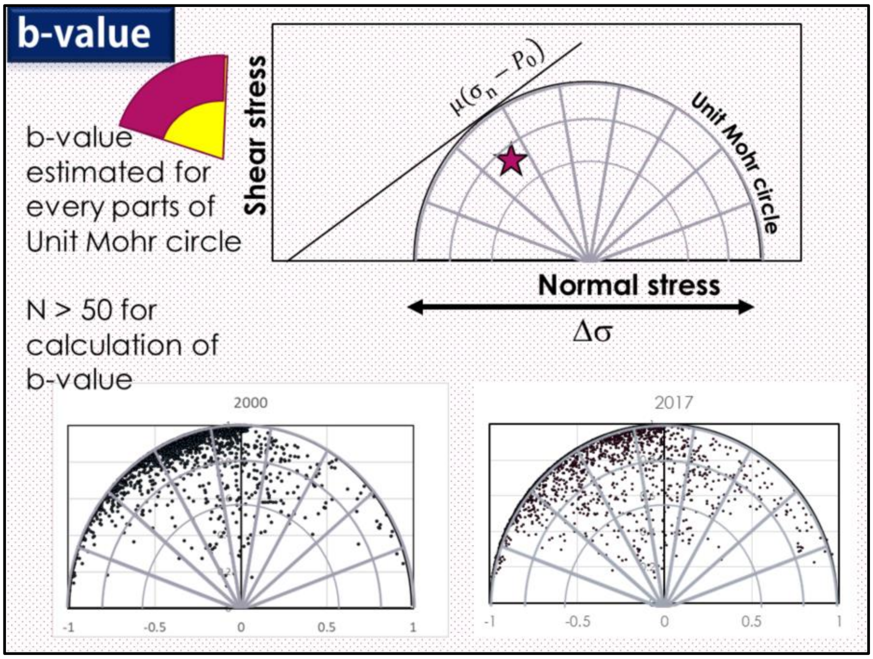

Next, we estimate b-values for frequency-size distribution at parts on the unit Mohr circle. Schematic illustration of this is displayed in the upper of the figure. Again, we show shear-normal stress plots for events in two observation periods at lower.
We estimate b-value for the part including larger than 50 events. Each part extend in angular direction until N greater than 50 events.

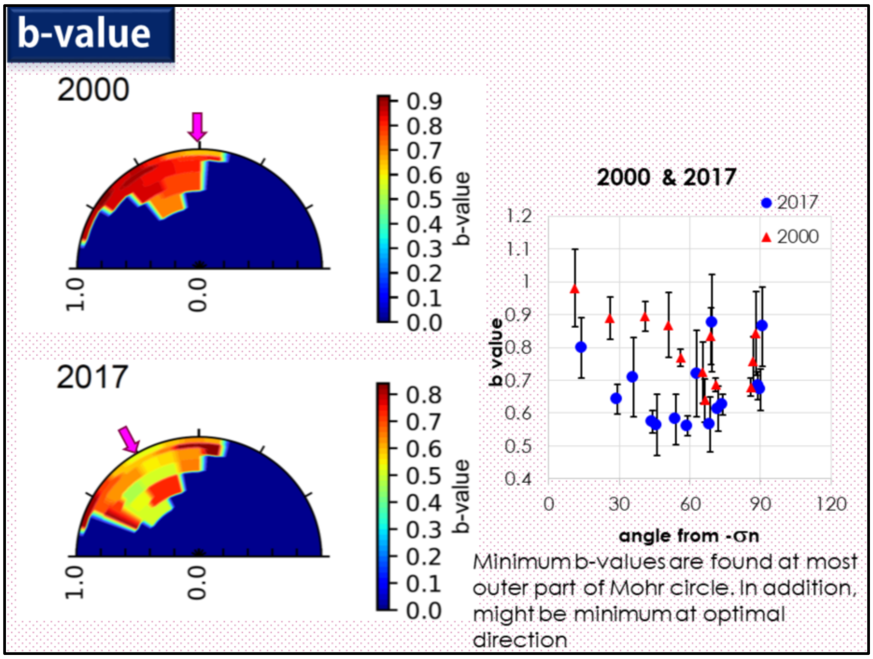

This figure shows b-value distribution on the unit Mohr circle. Upper and lower panes correspond to 2000 and 2017 observation, respectively. Right figure shows b-value with standard error for clockwise angle from horizontal axis of the Mohr circle.
Minimum positions are pointed by arrows.
For 2000 obs., minimum point is found at top of the circle. This means minimum b-value is revealed for the frequency-number distribution of fault plane that is oriented 45 degree from maximum and minimum principal stress axes.
On the other hand, it for 2017 observation is located at about 60 degree. At this part, fault plane with 30 degree from maximum principal stress is pronounced. Low b-value found inside of the Mohr circle is not reliable because of large error of estimation.
This result can be interpreted that large earthquake is relatively active for plane with friction coefficient of about under 0.2 for 2000 obs and 0.6 for 2017. It suggests that
1) At the minimum position of the Mohr circle, elastic energy can rise up until strength for the medium with internal friction. That's why large earthquake can be generated. Inside the Mohr circle, strength is low

because earthquake never occur without high pore pressure.
2) Friction coefficient vary from 2000 to 2017, implying it is recovered from just after earthquake occurrence.

Summary

- Strength – b-value relation obtained from precise focal mechanism data
  - b-value takes minimum value at probably optimum fault plane direction
  - Larger differential stress corresponds to smaller b-value
    - Higher fault strength generates larger earthquake
    - Fault strength decline maybe due to pore-fluid creates increasing b-value
  - $b = c\Delta\sigma \cdot F(\mu, \tau/\Delta\sigma, \sigma_n/\Delta\sigma)$: b-value could be affected by differential stress & degree of attainment to fault failuer
- Friction coefficient might be estimated from b-value distribution on a Mohr circle
  - In case that large earthquake is generated under maximum elastic energy supplied to a medium.
  - Friction coefficient change from 0.4 to 0.7 during 17 years (2017 – 2000)?

supplements

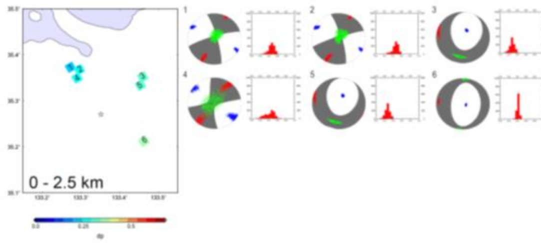

Figure A1. a) Estimated stress tensor and confidence ranges at each spatial bin at depth range of 0 – 2.5 km. Beach ball indicates the tensor in lower hemisphere. Blue, green and red dots indicate 95 % confidence range for the estimation. Histogram shows 95 % confidence range in stress ratio (s2-s3)/(s1-s3).

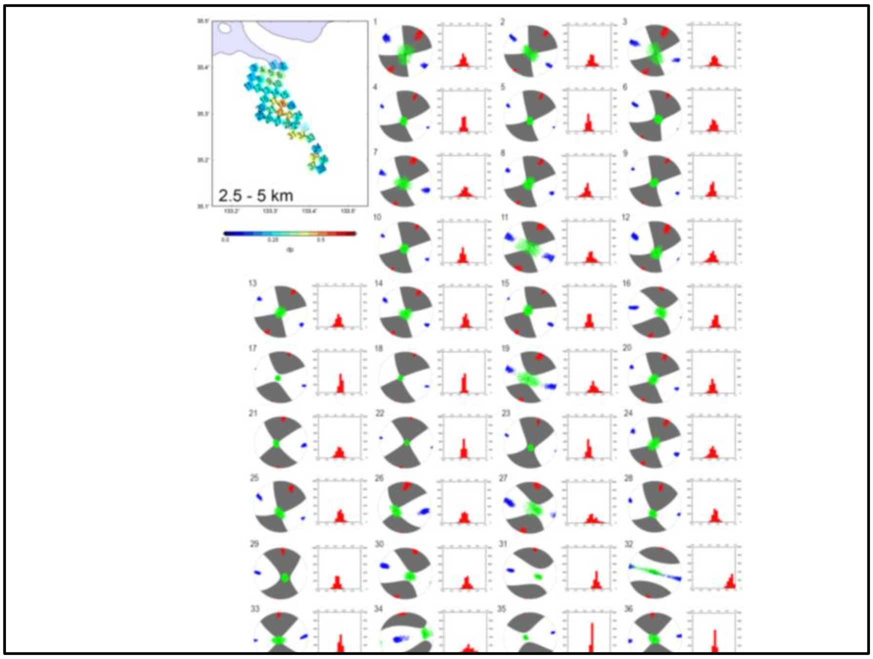

Figure A1 b) Same as a) except depth range of 2.5 – 5 km.

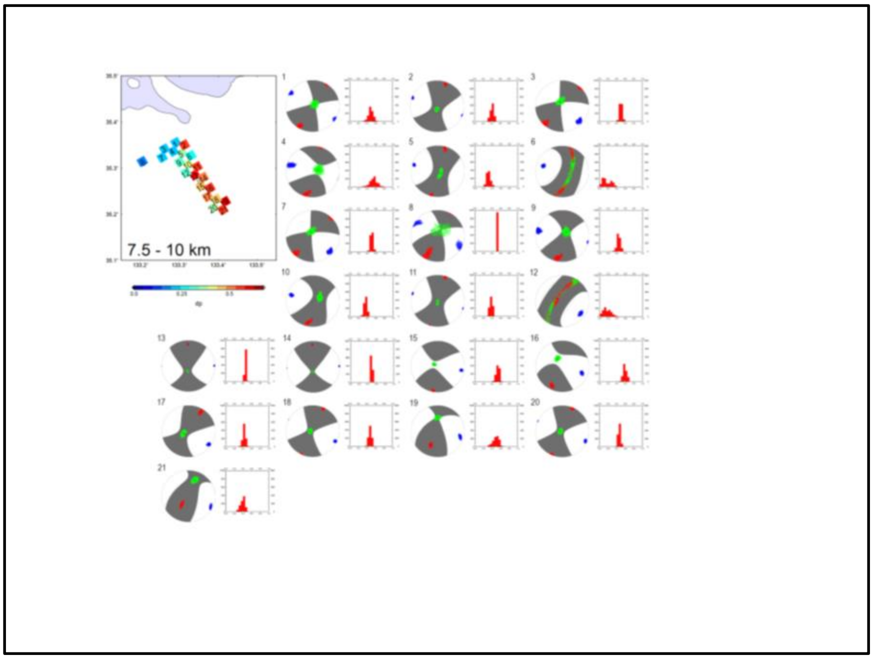

Figure A1 d) Same as a) except depth range of 7.5 – 10 km.

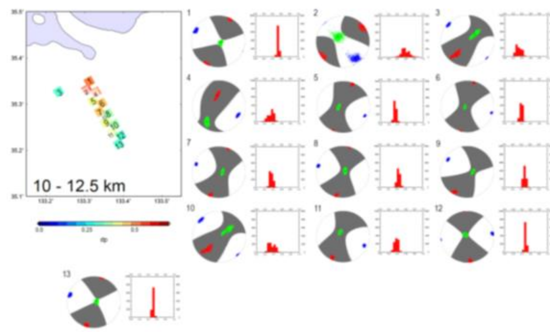

Figure A1 e) Same as a) except depth range of 10 – 12.5 km.

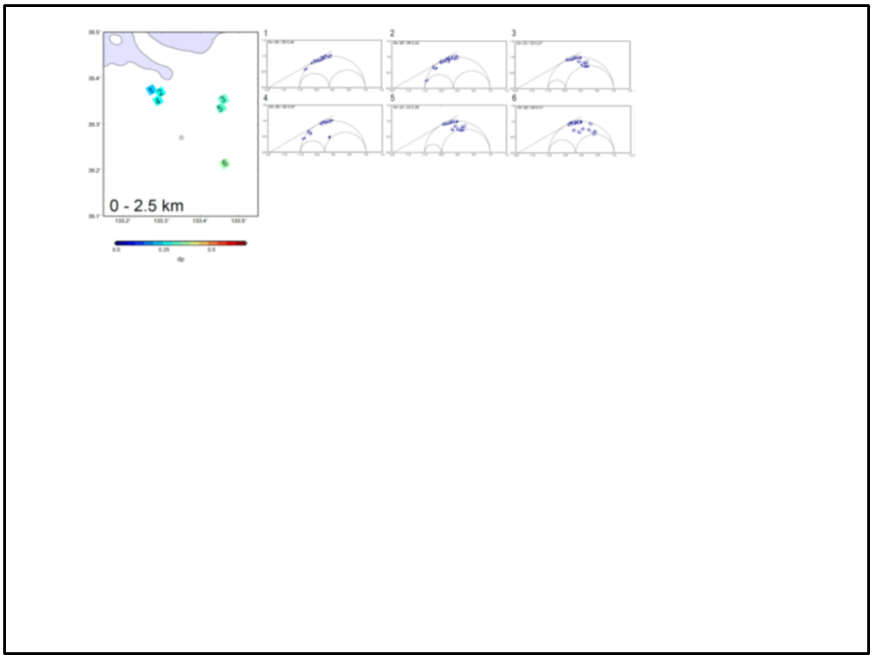

Figure A2. a)Relative shear and normal stress of each event plotted on a unit Mohr circle based on the estimated stress tensor for each spatial bin at 0 – 2.5 km depth range. Beach ball shows focal mechanism of the event.

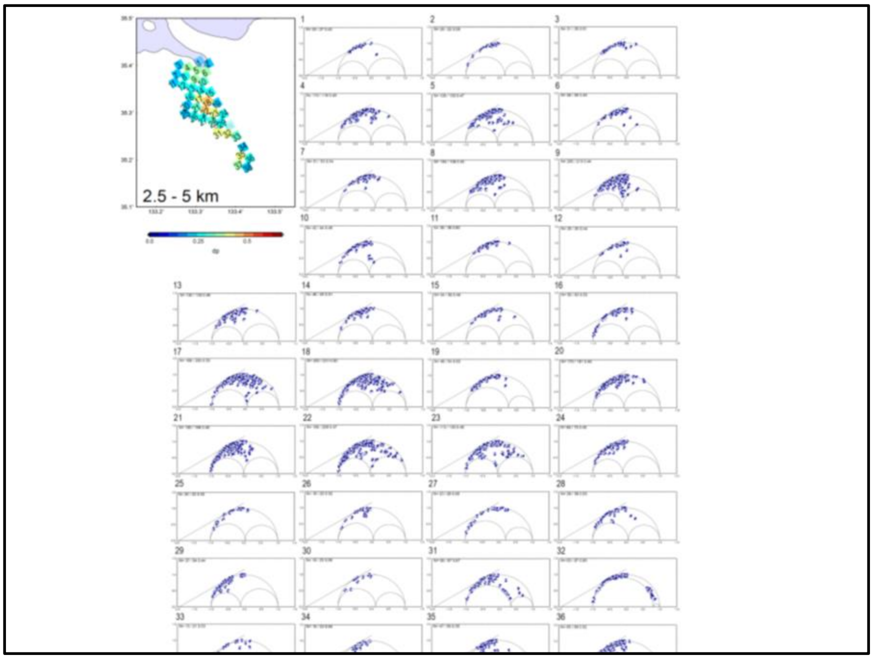

Figure A2 b) Same as a) except depth range of 2.5 – 5 km.

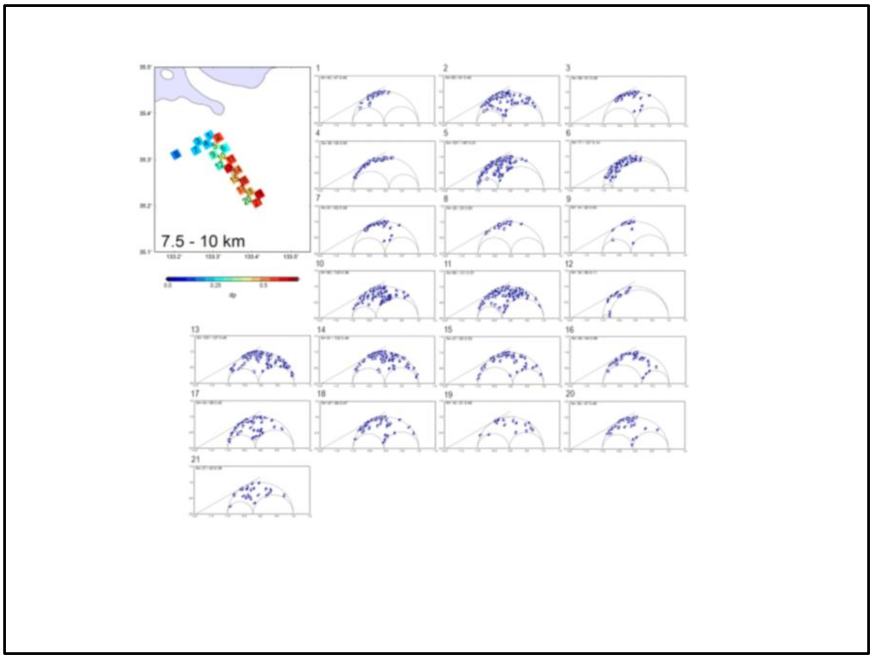

Figure A2 d) Same as a) except depth range of 7.5 – 10 km.

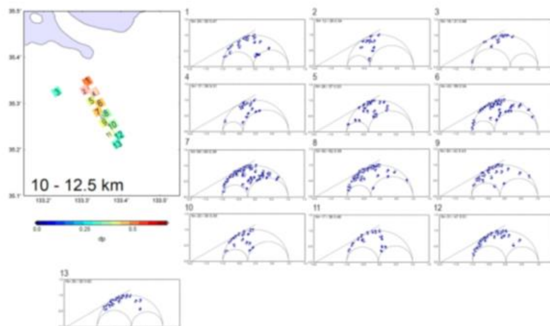

Figure A2 e) Same as a) except depth range of 10 – 12.5 km.

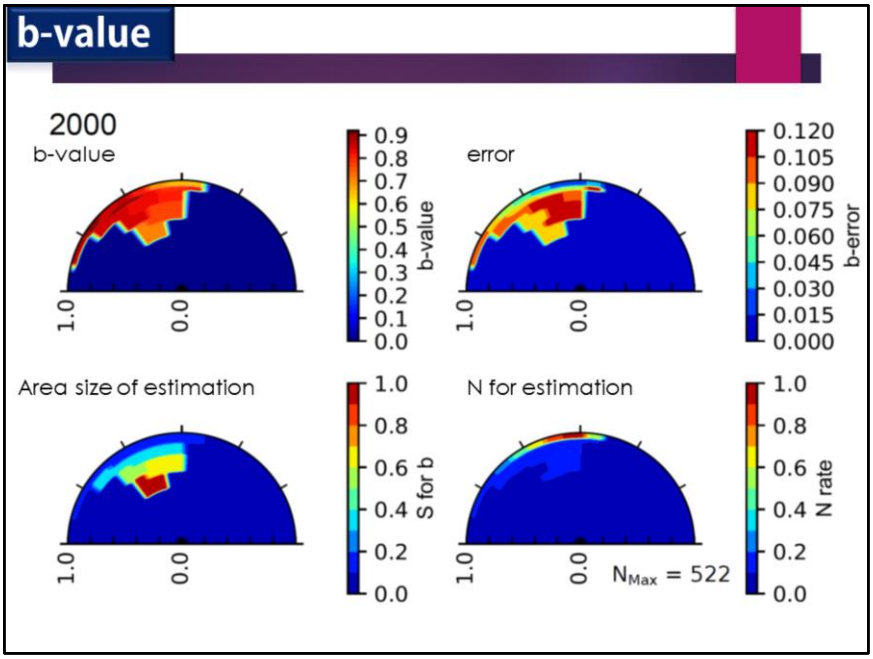

Fig. A3 a) b-value plot on the Mohr circle for data in 2000 observation. b-value, standard error, area size of estimation, number of event estimate are plotted.

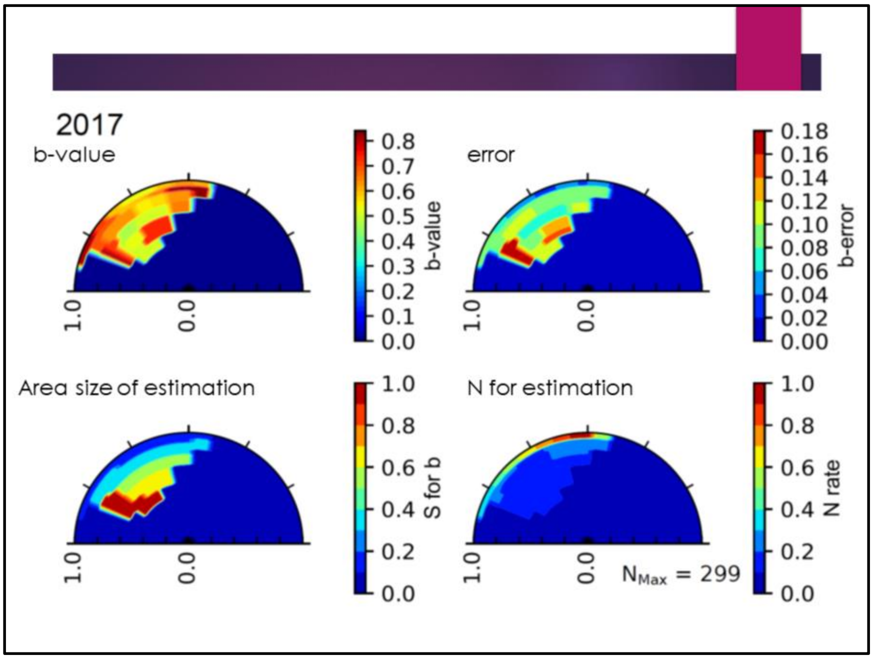

Fig. A3 b) Same as a) but for 2017 observation.